AUTOMATED C AND Si ISOTOPIC ANALYSIS OF PRESOLAR SiC GRAINS FROM THE INDARCH ENSTATITE CHONDRITE. E. Zinner[1], F. Gyngard[1], and L. R. Nittler[2], [1]Laboratory of Space Sciences and the Physics Department, Washington University in St. Louis, One Brookings Dr., St. Louis, MO 63130, USA., ekz@wustl.edu, [2]DTM, Carnegie Institution of Washington, 5241 Broad Branch Road, NW Washington, DC 20015, USA.

Introduction: In a previous study, we have used the NanoSIMS in a manual grain analysis mode to measure C, N, and Si isotopic ratios of presolar SiC grains in separate IH6 (grain diameters 0.25-0.65 µm) from the Indarch EH4 chondrite [1]. Here we report on automated measurements of grains from the IH6 separate.

Experimental: We used a recently developed automated, high-mass-resolution technique for the isotopic analysis of well separated grains in the NanoSIMS [2] to measure the C and Si isotopic ratios of 814 SiC and 50 Si_3N_4 grains from IH6. After presputtering of a 20×20 µm^2 area with a high primary beam current to implant Cs, simultaneous raster images of $^{12,13}C^-$ and $^{28,29,30}Si^-$ were obtained with a finely focused Cs^+ beam. Grains identified by a particle recognition algorithm were analyzed for their C and Si isotopic ratios by deflecting the primary beam onto them. N and Mg-Al isotopes were measures manually in subsequent analysis sessions.

Results: The Si and C isotopic ratios of all analyzed SiC grains and two Si_3N_4 grains of type X are shown in figures 1-4. The SiC grains comprise all types and the distribution of the isotopic ratios is very similar to that obtained from the previous NanoSIMS analysis of IH6 grain in manual grain mode [1].

Table 1 shows a comparison of the abundances of different grain types [3] from the present study and the

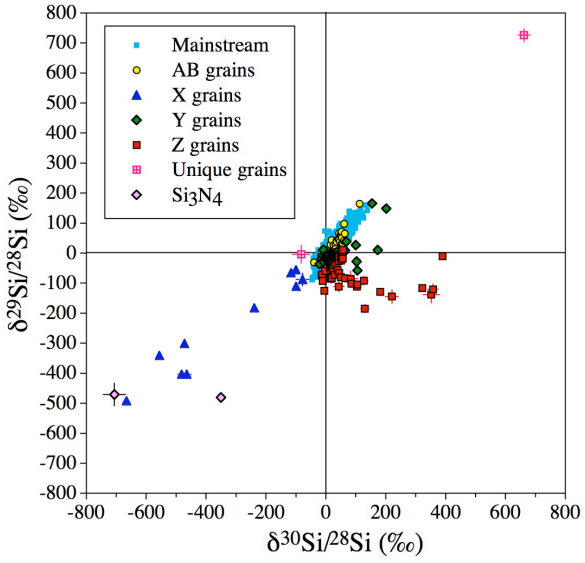

Figure 1

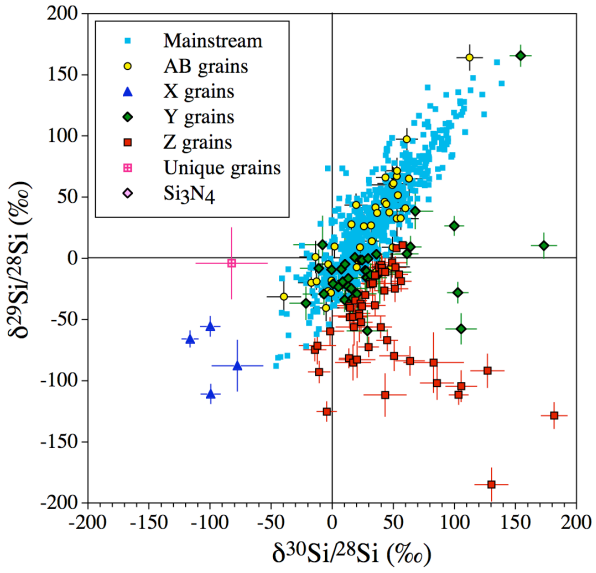

Figure 2

previous study made with the manual grain mode [1]. As can be seen, the abundances are identical within the statistical uncertainties. As has been observed before, the abundance of Y and Z grains, believed to originate in low-metallicity AGB stars, is much higher among small grains than among large SiC grains. This provides the opportunity to analyze isotopes of other elements in the otherwise rare Z grains, and Ti, Fe and Ni isotopes have been measured in Z grains from the IH6 separate [1, 4]. Most Si_3N_4 grains have close-to-solar Si isotopic ratios. Although C isotopic ratios measured in many of these grains are anomalous and cover a large range, as discussed before [1], it cannot be excluded that the C originates from tiny attached SiC grains. Thus, most Si_3N_4 grains likely have an origin in the solar system [5]. Exceptions are two Si_3N_4 grains of type X with large ^{28}Si excesses, indicative of a supernova origin.

Table 1. Abundances of grain types

Type	Number	Fraction %	Manual %
Mainstream	669	82.3	79.6
AB	39	4.8	4.9
X	10	1.2	1.5
Y	40	4.9	6.4
Z	54	6.6	7.6
Unique	2	0.2	
Total	814		548

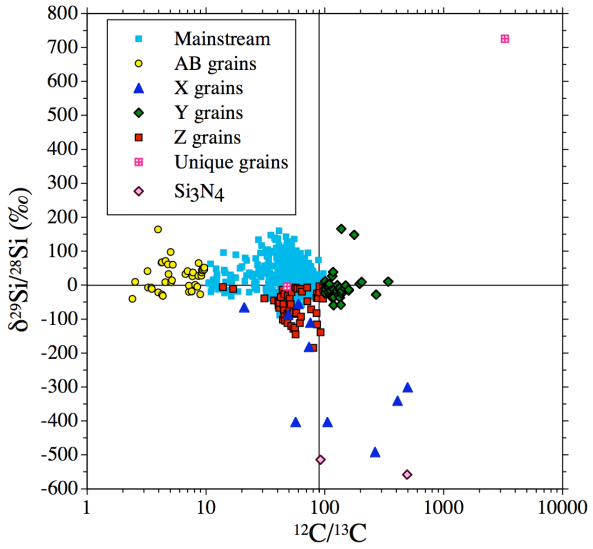

Figure 3

Two grains were classified as unique. One has a ^{30}Si deficit but the deviation from mainstream grains is marginal. The other grain, f2-1-1-7, has large excesses in ^{29}Si and ^{30}Si. Such grains are extremely rare. Two with even larger excesses have previously been identified. One, KJGP1-146-1 (δ^{29}Si = 2680 ‰, δ^{29}Si = 3290 ‰) is from Murchison SiC fraction KJG [6], the other, KC-5 (δ^{29}Si = 1280 ‰, δ^{29}Si = 1007 ‰), is a SiC subgrain within a high-density graphite grain from Murchison fraction KFC1 [7]. Both have higher than solar ^{12}C/^{13}C (844 and 240) and lower than solar ^{14}N/^{15}N (213 and 120) ratios.

To obtain more information, we measured the N and Mg-Al isotopic ratios of the unique grain f2-1-1-7 and the two type X Si_3N_4 grains. Before doing so we

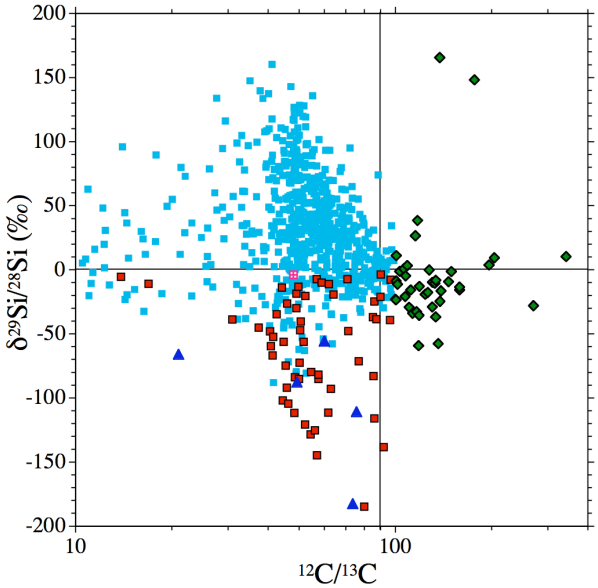

Figure 4

obtained C and Si isotopic images of 2×2 μm^2 areas around the grains and sputtered nearby grains away with the Cs beam, similar to what has been done before with oxide grains [8]. For grain f2-1-1-7, this resulted in an increase from the original ^{12}C/^{13}C = 175, δ^{29}Si = 485 ‰, and δ^{30}Si = 435 ‰ to the values shown in Table 2, demonstrating that the original automatic measurement was affected by beam overlap onto an adjacent grain. The ^{12}C/^{13}C ratio in the table is still a lower limit, as the grain is small and contamination with isotopically normal C would decrease the ratio.

The ^{14}N/^{15}N and inferred ^{26}Al/^{27}Al ratios shown in the table were obtained from the thus cleaned grains. The ^{15}N excesses and high ^{26}Al/^{27}Al ratios in the Si_3N_4 grains confirm a SN origin. Grain f2-1-1-7 has also a ^{15}N excess. The most likely origin of this unique grain is also a Type II SN. The He/C zone of a SN has the C, N, and Si isotopic signatures seen in this grain: ^{29,30}Si excesses are predicted to result from neutron capture, He burning produces ^{12}C and results in very high ^{12}C/^{13}C ratios, and ^{15}N is produced by neutrino reactions on O, especially in the lowest layers of the He/C zone. By mixing layers from the bottom (needed to obtain large enough ^{29,30}Si excesses) and middle of the He/C zone and the He/N zone of the 15 $M_\odot$ SN model by Rauscher et al. [9], we can reproduce the C, N, and Si isotopic ratios of grain f2-1-1-7. The only discrepancy is the ^{26}Al/^{27}Al ratio, for which the prediction of the SN mixing model is higher by about a factor 5 than the measured ratio. Contamination by terrestrial Al on the sample mount would lower the inferred ratio and cannot be excluded; however, the grain was consumed during the Mg-Al measurement and was too small to investigate this possibility.

We thank Sachiko Amari and Cristine Jennings for preparation of the Indarch IH6 separate.

Table 2. Isotopic ratios of selected grains

Grain	^{12}C/^{13}C	^{14}N/^{15}N	δ^{29}Si (‰)	δ^{30}Si (‰)	^{26}Al/^{27}Al (10^{-3})
f2-1-1-7	3270±816	111±9	726±19	662±21	4.5±1.1
e4-1-1-36	92±33	124±11	-514±14	-400±12	126±9
gm-test2-4-3	493±250	52±3	-558±37	-720±37	86±6

References: [1] Zinner E. et al. (2007) *GCA 71*, 4786-4813. [2] Gyngard F. et al. (2009) *LPS XL*, Abstract #1386. [3] Hoppe P. and Ott U. (1997) in: *Astrophysical Implications of the Laboratory Study of Presolar Materials*, (eds. T. J. Bernatowicz and E. Zinner), pp. 27-58. [4] Hynes K. M. et al. (2009) *Meteoritics & Planet. Sci. 44*, A96. [5] Alexander C. M. O'D. et al. (1994) *Meteoritics 29*, 79-85. [6] Amari S. et al. (1999) *ApJ 517*, L59-L62. [7] Croat T. K. and Stadermann F. J. (2008) *LPS XXXIX,* Abstract #1739. [8] Zinner E. and Gyngard F. (2009) *LPS XL*, Abstract #1046. [9] Rauscher T. et al. (2002) *ApJ 576*, 323-348.